ORIGINAL PAPER

Y. J. Leng · S. H. Chan · K. A. Khor · S. P. Jiang

$(La_{0.8}Sr_{0.2})_{0.9}MnO_3$–$Gd_{0.2}Ce_{0.8}O_{1.9}$ composite cathodes prepared from $(Gd, Ce)(NO_3)_x$-modified $(La_{0.8}Sr_{0.2})_{0.9}MnO_3$ for intermediate-temperature solid oxide fuel cells

Abstract Development of high performance cathodes with low polarization resistance is critical to the success of solid oxide fuel cell (SOFC) development and commercialization. In this paper, $(La_{0.8}Sr_{0.2})_{0.9}MnO_3$ (LSM)–$Gd_{0.2}Ce_{0.8}O_{1.9}$(GDC) composite powder (LSM ~70 wt%, GDC~30 wt%) was prepared through modification of LSM powder by $Gd_{0.2}Ce_{0.8}(NO_3)_x$ solution impregnation, followed by calcination. The electrode polarization resistance of the LSM–GDC cathode prepared from the composite powder was ~0.60 Ω cm^2 at 750 °C, which is ~13 times lower than that of pure LSM cathode (~8.19 Ω cm^2 at 750 °C) on YSZ electrolyte substrates. The electrode polarization resistance of the LSM–GDC composite cathode at 700 °C under 500 mA/cm^2 was ~0.42 Ω cm^2, which is close to that of pure LSM cathode at 850 °C. $Gd_{0.2}Ce_{0.8}(NO_3)_x$ solution impregnation modification not only inhibits the growth of LSM grains during sintering but also increases the triple-phase-boundary (TPB) area through introducing ionic conducting phase $(Gd,Ce)O_{2-\delta}$, leading to the significant reduction of electrode polarization resistance of LSM cathode.

Keywords Intermediate-temperature SOFC · Composite cathode · Impregnation · Polarization resistance

Introduction

Solid oxide fuel cell (SOFC) has reached a stage in its development where commercial exploitation of this clean technology for power generation is now seen possible. Lowering operating temperature from the traditional 1,000 °C to an intermediate temperature range of 600–800 °C can not only reduce the degradation of fuel cell/stack components and prolong the lifetime of fuel cell systems but also widen materials selection. In addition, cheap stainless steel materials can be used as interconnect at intermediate temperatures. However, with lowering operating temperature, two problems should be solved; one is the increase of electrolyte resistance, and the other is the increase of electrode polarization loss/resistance. The former can be solved by reducing the thickness of yttria-stabilized zirconia (YSZ) electrolyte to 5–20 μm [1–3], and/or adopting alternative electrolyte materials with higher ionic conductivity at intermediate temperatures than YSZ, such as doped lanthanum gallate (LaGaO₃) [4–7] and doped ceria [8–11]. Therefore, development of high performance electrodes with low polarization losses and high stability is critical to the successful development and commercialization of intermediate temperature SOFCs technology.

LSM is the commonly used cathode material for high temperature SOFCs due to its high electronic conductivity, high catalytic activity at high temperature, and good compatibility with YSZ electrolyte [12]. However, its low ionic conductivity and high activation energy limit its application as cathode material for intermediate temperature SOFCs. There are several strategies for utilizing oxide cathodes successfully in the intermediate temperature (600–800 °C) region. One option is to find alternative cathodes with higher catalytic activity at lower temperatures, particularly cobaltite-based cathodes. For example, (La,Sr)(Co,Fe)O₃-based cathodes have been optimized for the application in intermediate temperature SOFC, especially with ceria-based electrolyte[13, 14]. However, there are several problems regarding their use in intermediate temperature SOFCs with thin film YSZ electrolyte including their thermal expansion coefficient mismatch with YSZ and high reactivity of dopant oxide with YSZ. Another option is

Y. J. Leng (✉) · S. H. Chan · K. A. Khor · S. P. Jiang
Fuel Cell Strategic Research Programme,
School of Mechanical and Aerospace Engineering,
Nanyang Technological University, 50 Nanyang Avenue,
Singapore 639798, Singapore
E-mail: myjleng@ntu.edu.sg
Tel.: +65-6790-4349
Fax: +65-6791-1859

to improve single-phase LSM cathode performance in SOFCs. One commonly used means is to add an ionically conducting second phase such as YSZ [15–17] or GDC [18–20] to LSM, which is the electronically conducting cathode material, to form a composite cathode. Murry et al. [18] mixed physically $Gd_{0.2}Ge_{0.8}O_{2-x}$ (GDC) powder with $La_{0.8}Sr_{0.2}MnO_3$ (LSM) powder to form LSM–GDC composite cathodes and found that the polarization resistance of LSM–GDC (50:50 wt%) composite cathode on YSZ electrolyte was 1.06 $\Omega\,cm^2$ at 700 °C, about $2 \sim 3$ times lower than that of LSM-YSZ (50:50 wt%) composite cathode (i.e., 2.49 $\Omega\,cm^2$). Xia et al. [19] prepared LSM–GDC (50:50 wt%) composite cathode via a sol–gel process and found the polarization resistance of the composite cathode was only 0.28 $\Omega\,cm^2$ at 700 °C. The authors attributed its high performance to the unique microstructure of the cathode: very small grain size, high porosity and large specific surface area. However, the fabrication process is quite complex and time-consuming, consisting of about ten times' repeated coating–drying–firing procedure. Recently in our group, nano-size GDC particles have been successfully introduced into the LSM cathode by ion-impregnation method and a pretty low cathode polarization resistance of ~0.72 $\Omega\,cm^2$ at 700 °C has been achieved [20]. Though the result was encouraging, ion-impregnation treatment of LSM cathode is also a time-consuming process. This method requires repeated ion-impregnation/sintering process for three to five times to obtain sufficient amount of ionic conductor in the cathode structure. In addition, it is difficult to determine the mass/volume fraction of GDC impregnated into the cathode.

In the study, a simple and cost-effective method is introduced for fabricating the LSM–GDC composite cathode. In this method, LSM powder is modified by $Gd_{0.2}Ce_{0.8}(NO_3)_x$ impregnation, followed by calcination. With this method, only a single ion-impregnation/calcination cycle is required and the mass fraction of GDC powder in the composite cathode can be easily determined or controlled.

Experimental

Preparation of LSM–GDC composite powder

$(La_{0.8}Sr_{0.2})_{0.9}MnO_3$ powder was synthesized by a coprecipitation wet chemical process and coarsened at 1,000 °C. The impregnation solution of 20 mol% $Gd(NO_3)_3$ + 80 mol% $Ce(NO_3)_3$ $(Gd_{0.2}Ce_{0.8}(NO_3)_x)$ was prepared from $Gd(NO_3)_3\cdot6H_2O$ (99.9%, Aldrich Chemical Company) and $Ce(NO_3)_3\cdot6H_2O$ (99.9%, Aldrich Chemical Company). The metal-ion concentration of the solution was 3 mol/L. The pH level of 3 mol/L $Gd_{0.2}Ce_{0.8}(NO_3)_x$ solution was ~3. The LSM–GDC composite powder was prepared by placing LSM powder in an appropriate amount of 3 mol/L $Gd_{0.2}Ce_{0.8}(NO_3)_x$ solution, stirring for 12 h and letting the solution soak into LSM powder in open air, then followed by evaporating the water and firing the mixture at 850 °C for 2 h. After heat-treatment of $Gd_{0.2}Ce_{0.8}(NO_3)_x$ nitrate salt solution, $Gd_{0.2}Ce_{0.8}O_{2-\delta}$-type oxide phase was formed. Our previous study about micro modeling of composite electrode showed that, for a cathode made of YSZ and strontium-doped $LaMnO_3$ (LSM), the optimum YSZ volume fraction (ψ_{YSZ}) with minimum polarization resistance depends on the ratio of average grain size of YSZ to that of LSM, varying from $\psi_{YSZ} = 0.24$ for $r_{io}/r_{el} = 0.2$ to $\psi_{YSZ} = 0.55$ for $r_{io}/r_{el} = 1$ and $\psi_{YSZ} = 0.81$ for $r_{io}/r_{el} = 5$ [21]. The results imply that if one could impregnate nano-size ionic conducting material in the LSM structure, the amount required in the composite electrode can be significantly less. Therefore, in this study we set the amount of GDC in the LSM–GDC composite powder as ~30 wt%. The calculated volume fraction of GDC is $\sim28\%$.

Fabrication of LSM–GDC composite cathodes

YSZ electrolyte substrates were prepared from 8 mol% Y_2O_3 doped ZrO_2 powder (TZ-8YS, Tosoh, Japan) by isostatic pressing, followed by firing at 1,500 °C for 4 h. On the other hand, GDC electrolyte substrates were prepared from nano-size $Gd_{0.1}Ce_{0.9}O_{1.95}$ powder (Nextech, USA) by isostatic pressing, followed by firing at 1,350 °C for 4 h. Both electrolyte substrates achieved a density better than 95%. The dimensions of the substrates were ~19 mm in diameter for YSZ discs, ~17 mm in diameter for GDC discs, both ~0.75 mm in thickness.

The LSM–GDC composite powder was mixed with polyethylene glycol 400 to form the cathode paste. The paste was applied onto the electrolyte substrate by screen-printing, followed by sintering at 1,050–1,250 °C for 2 h. Electrode coating thickness was 20–30 μm with an effective area of 0.5 cm^2. Pt paste (Ferro Corporation, USA) was painted on the opposite side of the working electrode to serve as counter and reference electrodes. The counter electrode was symmetrical to the working electrode and a reference electrode was painted as a ring around the counter electrode. The gap between counter electrode and reference electrode was ~3 mm. Pt mesh was used as a current collector for both working electrode and counter electrode, and two Pt wires were spot-welded on the current collector to serve as current and voltage probes separately.

Electrochemical test and structure characterization

The electrode performance of LSM and LSM–GDC composite cathode was measured in air at 650–850 °C in a three-electrode system using electrochemical impedance spectroscopy (EIS). EIS was performed under open-circuit or bias current using an Autolab electrochemical system (PGSTAT30/FRA, Netherlands). The impedance

measurement was conducted in the frequency range of 0.1 Hz to 100 kHz with signal amplitude of 10 mV for the impedance measurement under open-circuit and 5 mA for the impedance measurement under bias current. Scanning electron microscopy (SEM, JEOL 6500) was used to observe the morphology and microstructure of cathodes, and X-ray powder diffratometer (XRD) with Cu-Kα radiation was used to characterize the phase of the LSM–GDC composite powder.

Results and discussion

Materials characterization and cathode microstructure

Figure 1 shows the XRD patterns of as-prepared LSM–GDC composite powder and pure LSM powder. The presence of the CeO_2-type phase in the composite powder was detected at $2\theta = 28.4$, 47.3, and 56.2, which were ascribed to the cubic fluorite phase of $(Gd, Ce)O_{2-\delta}$. The analysis confirmed that the LSM–GDC composite powder was actually formed by the mixture of GDC and LSM phases.

Figure 2 shows SEM photos of the top-view of cathodes made of the LSM–GDC composite powder sintered at 1,050, 1,150 and 1,250 °C for 2 h on their respective YSZ electrolyte substrates. For comparison, SEM photo of the pure LSM cathode is also shown. During the heat treatment after the impregnation, some GDC particles may deposit on the surface of LSM grains, while some may deposit between the LSM grains. With increasing sintering temperature from 1,050 °C to 1,250 °C (Fig. 2a to 2c), the grain size of LSM in the LSM–GDC composite cathode increases. However, even at sintering temperature 1,250 °C (Fig. 2c), the

grain size of LSM in the LSM–GDC composite cathode is still smaller than that in pure LSM cathode sintered at 1,150 °C (Fig. 2d). For example, the average size of LSM grains in the LSM–GDC composite cathode sintered at 1,150 °C and 1,250 °C was 0.47 ± 0.02 μm and 0.66 ± 0.04 μm, ∼ 2.3 and ∼1.5 times smaller than that in pure LSM cathode sintered at 1,150 °C (1.06 ± 0.11 μm), respectively. This implies that GDC particles deposited on the surface of LSM or between LSM grains may be the cause of inhibiting the grain growth of LSM. Intuitively, smaller grain size of LSM will increase the TPB area for oxygen reduction, thus reducing the cathode polarization.

Figure 3 shows SEM photos of the cross-sectional view of cathodes made of the LSM–GDC composite powder sintered at 1,050 and 1,150 °C for 2 h on YSZ electrolyte substrates (Figs. 3a, b) and sintered at 1,150 and 1,250 °C for 2 h on GDC electrolyte substrates (Figs. 3c, 3d). In the case of sintering at 1,050 °C (Fig. 3a), the LSM–GDC composite grains appeared to have sintered well and bonded well at cathode/YSZ interface. However, when sintering temperature was increased from 1,050 °C (Fig. 3a) to 1,150 °C (Fig. 3b), partial detachment of cathode from YSZ electrolyte substrate was observed. Similarly, when sintered at 1,250 °C, the LSM–GDC composite cathode was fully detached from YSZ substrate (not shown in this paper), although the LSM–GDC composite grains were sintered well with each other (as shown in Fig. 2c). The reasons for the detachment of LSM–GDC composite cathode from YSZ electrolyte under sintering temperature above 1,200 °C are unclear at this stage. A possible explanation is the mismatch of thermal expansion coefficients (TEC) between the LSM–GDC composite and YSZ (Note that the TEC of GDC and YSZ are, respectively,

Fig. 1 X-ray diffraction patterns of as-prepared pure LSM powder and LSM–GDC composite powder: **a** LSM–GDC composite powder, **b** pure LSM powder
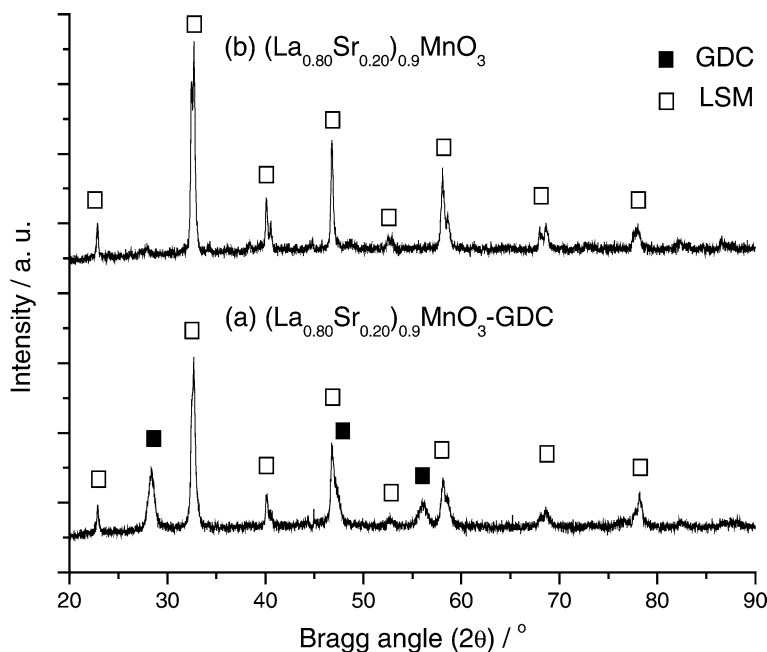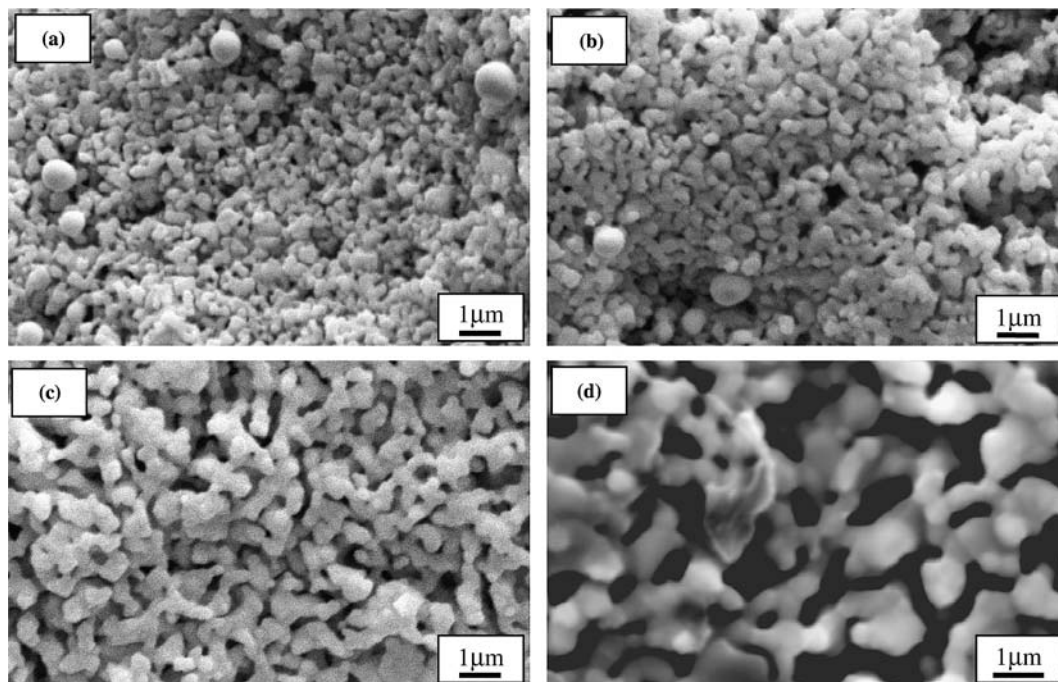
Fig. 2 SEM micrographs of the surface top view of the cathodes prepared from LSM–GDC composite powder and pure LSM powder: **a** LSM–GDC, sintered at 1,050 °C; **b** LSM–GDC, sintered at 1,150 °C; **c** LSM–GDC, sintered at 1,250 °C; and **d** pure LSM, sintered at 1,150 °C (sintering time: 2 h)

12.5×10^{-6} K^{-1} and 10.5×10^{-6} K^{-1}) and large shrinkage of LSM–GDC composite cathode at sintering temperature above 1,200 °C. Nonetheless, on GDC electrolyte substrate, for both cases of sintering at 1,150 and 1,250 °C, the LSM–GDC composite grains were bonded well with the GDC substrates.
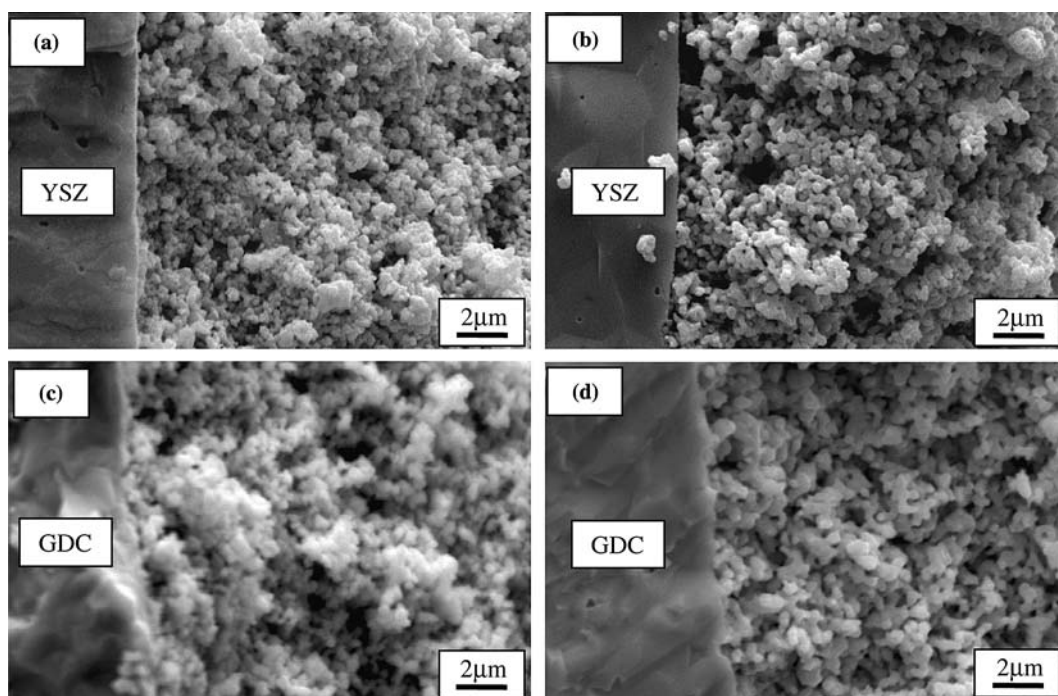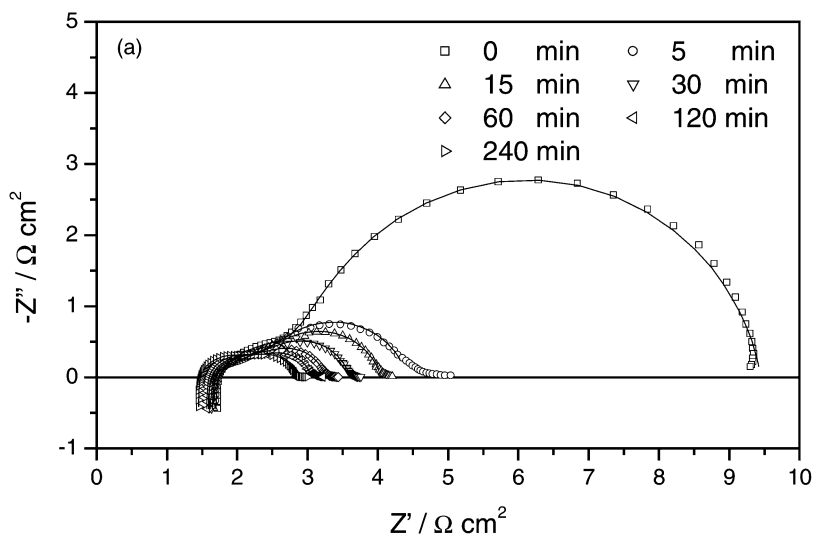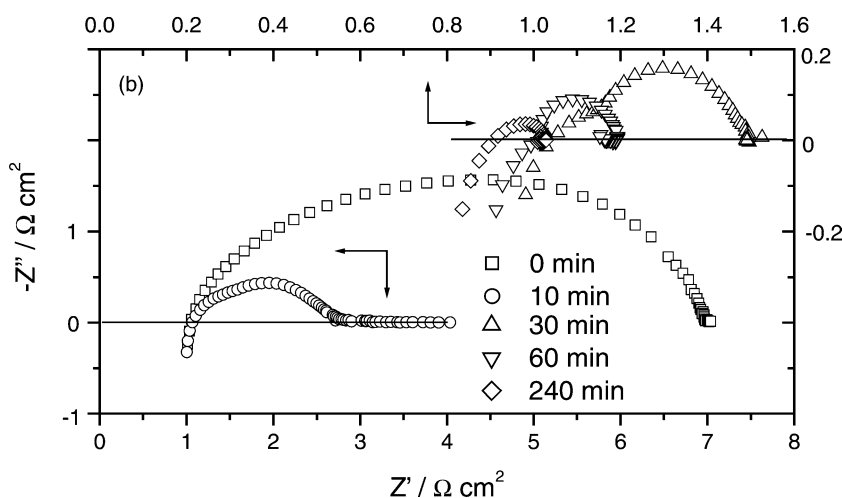

Fig. 3 SEM micrographs of the cross-sectional view of the cathodes prepared from LSM–GDC composite powder on YSZ or GDC electrolyte substrate: **a** on YSZ, sintered at 1,050 °C; **b** on YSZ, sintered at 1,150 °C; **c** on GDC, sintered at 1,150 °C; and **d** on GDC, sintered at 1,250 °C (sintering time: 2 h)

Pure LSM

LSM-GDC composite cathode

Impedance of LSM–GDC composite cathode under open-circuit condition

Figure 4 shows the initial impedance response of a cathode made of (a) pure LSM powder (sintered at 1,150 °C for 2 h and measured at 850 °C) and (b) the LSM–GDC composite powder (sintered at 1,150 °C for 2 h and measured at 800 °C) on YSZ electrolyte as a function of cathodic current passage time at 200 mA/cm^2 in air. The impedance spectra of pure LSM cathode show a typical initial behavior of freshly prepared LSM cathode [22, 23]. Before passing cathodic current, the initial electrode behavior was characterized by high electrode polarization resistance (R_p) ($\sim$7.7 Ω cm^2 at 850 °C). With the passing of the cathodic current, R_p was reduced rapidly. As reported by Jiang et al. [22], the high initial electrode polarization resistance is most likely due to the presence of surface species such as SrO$_2$ and MnO$_x$ originally enriched at the LSM electrode surface. The cathodic current treatment can possibly remove this surface resistive layer. Structural change induced by the cathodic current polarization could also contribute to the improvement of the initial polarization performance of LSM electrodes [23]. LSM–GDC composite cathode showed much better performance than that of pure LSM cathode (Fig. 4b). R_p for the LSM–GDC composite cathode was $\sim$6.0 Ω cm^2 at 800 °C (note that due to the effect of inductance at high frequency, the fitted ohmic resistance is slightly smaller than high frequency intercept), which was smaller than $\sim$7.7 Ω cm^2 of pure LSM cathode at 850 °C. With increasing cathodic passage time at 200 mA/cm^2 for 4 h, the electrode polarization resistance decreased significantly, from $\sim$6.0 Ω cm^2 to $\sim$0.21 Ω cm^2 at 800 °C. This indicates that there was an activation effect of cathodic current passage on the performance of the LSM–GDC composite cathode. This activation effect might be due to the microstructural change of the LSM–GDC

Fig. 5 Impedance spectra at OCV measured at 750 °C in air of the cathodes prepared from LSM–GDC composite powder and pure LSM powder
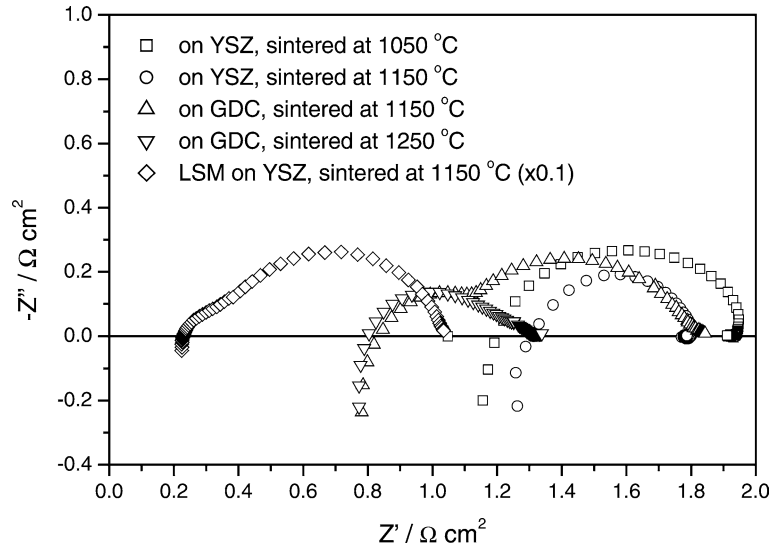
composite cathode. During impregnation and heat treatment, some GDC particles may cover the surface of LSM grains to form a thin layer of GDC, thus the electronic conducting path of the freshly-prepared LSM–GDC composite cathode might not be effectively established. Cathodic current passage might lead to breaking of GDC layer, which is helpful to establish the electronic and ionic conducting paths, thus improving the cathode performance. Further work is underway to understand the detailed mechanism of activation effect of cathodic current passage on the performance of the LSM–GDC composite cathode.

Figure 5 shows the impedance of the LSM–GDC composite cathode and LSM cathode measured at 750 °C, under the open circuit condition after cathodic current passage for 4 h. Results show that the electrode polarization resistance of the LSM–GDC composite

cathode sintered at 1,150 °C on YSZ electrolyte was ∼0.60 Ω cm^2, about 37% lower than that sintered at 1,050 °C on YSZ electrolyte (∼0.95 Ω cm^2); while the electrode polarization resistance of the LSM–GDC composite cathode sintered at 1,250 °C on GDC electrolyte was ∼0.68 Ω cm^2, about 38% lower than that sintered at 1,150 °C on GDC electrolyte (∼1.10 Ω cm^2). The electrode polarization resistance measured at 750 °C of LSM–GDC composite cathode sintered at 1150 °C on YSZ electrolyte in this study was close to that of LSM–GDC (50:50 wt%) composite cathode (i.e. ∼0.49 Ω cm^2 at 750 °C) prepared by physically mixing method [18]. LSM–GDC composite cathode in this study showed higher electrode polarization resistance than that prepared via sol-gel process (i.e. ∼0.16 Ω cm^2 at 750 °C) [19]. However, the latter was sintered at very low temperature (∼800 °C for 4 h) or test in situ after

Fig. 6 Electrode polarization resistance of cathodes (sintered at 1,050 °C∼1,250 °C for 2 h) prepared from LSM–GDC composite powder and pure LSM powder as a function of temperature
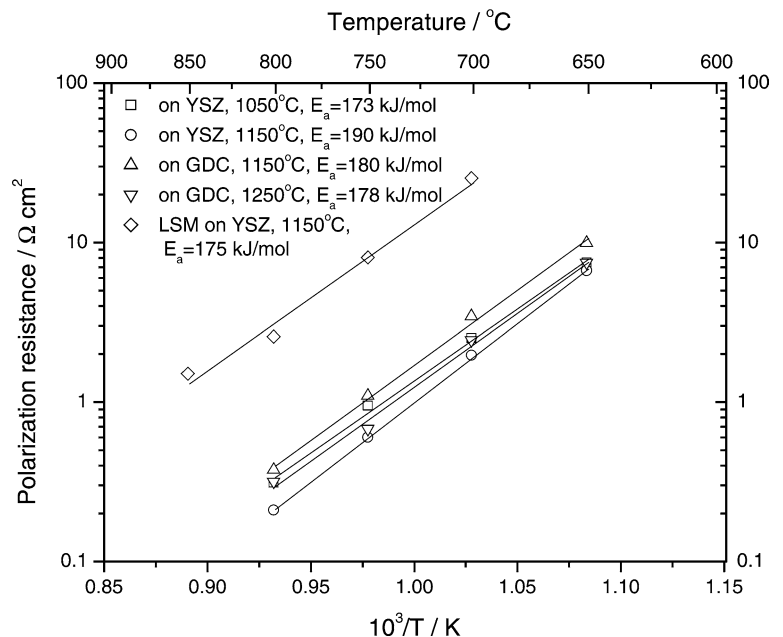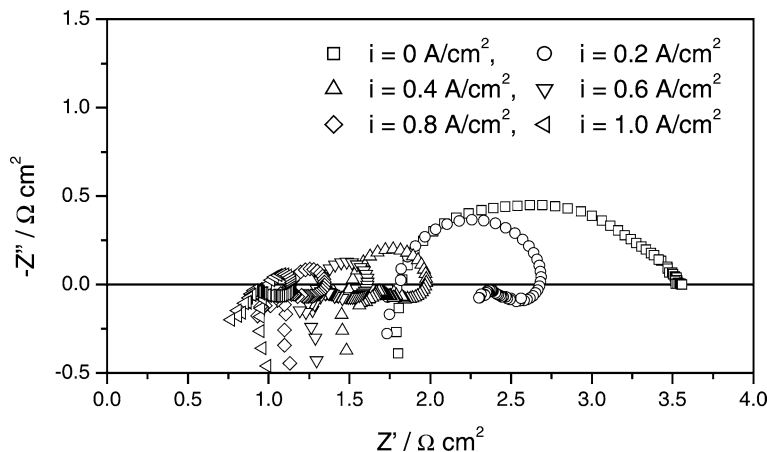
Fig. 7 Impedance spectra measured using AC current (AC = 5 mA) method measured at 700 °C in air of the cathodes (sintered at 1,150 °C for 2 h) prepared from LSM–GDC composite powder as a function of bias current density

calcining at 600 °C, which may lead to the performance degradation when operating at 750 °C for a long time. High sintering temperature (~1,150 °C) may increase the long-term stability of the LSM–GDC composite cathode in this study. Compared to pure LSM cathode sintered at 1,150 °C for 2 h on YSZ electrolyte substrate (~8.19 Ω cm^2 at 750 °C), the LSM–GDC composite cathodes show 7~13 times lower polarization resistance. Not only does the $(Gd,Ce)O_{2-\delta}$ particles deposited on the LSM grains inhibit the growth of LSM grains, but also the addition of $(Gd,Ce)O_{2-\delta}$ particles between LSM grains extends the reaction zone into cathode bulk, resulting in a significant increase of the electrochemical activities of LSM-based cathode for O_2 reduction.

Figure 6 shows electrode polarization resistance of the LSM–GDC composite cathodes under different sintering conditions as a function of operating temperature. For comparison, electrode polarization resistance of pure LSM cathode as a function of temperature is also shown in the figure. Results show that the activation energy of electrode polarization resistance of the

LSM–GDC composite cathode is almost independent of the sintering temperature and electrolyte substrates, ranging from 173 kJ/mol to 190 kJ/mol, which is close enough to that of pure LSM cathode (~175 kJ/mol). The study suggests that the LSM–GDC composite cathodes should have similar oxygen reduction mechanism as pure LSM cathode.

Characterization of cathode performance using impedance spectroscopy under bias current density

To obtain an accurate polarization curve, correction of the ohmic drop is needed. Ohmic resistance is often obtained from the high frequency intercept on the real axis of impedance plot measured under open-circuit condition. Figure 7 shows the impedance of LSM–GDC composite cathode measured at 700 °C as a function of bias current density. Results show that with increasing bias current density, the electrolyte ohmic resistance decreases. The reasons for the decrease of ohmic resistance with increasing bias current density are

Fig. 8 Polarization curve and electrode polarization resistance (R_p) and ohmic resistance (R_{ohm}) measured at 700 °C in air of cathodes (sintered at 1,150 °C for 2 h) prepared from LSM–GDC composite powder as a function of bias current density
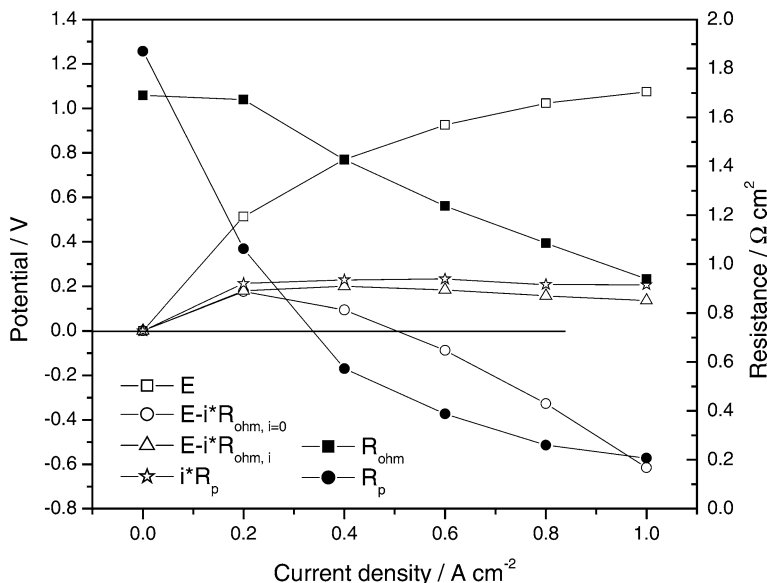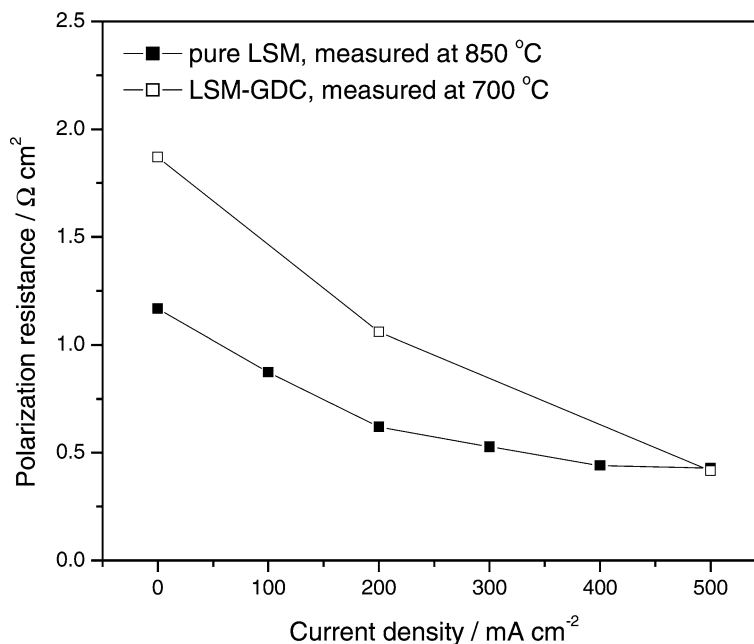
Fig. 9 Electrode polarization resistance of cathodes (sintered at 1,150 °C for 2 h) prepared from LSM–GDC composite powder and pure LSM powder as a function of bias current density

unclear at this stage. This phenomenon is probably due to local heating, causing the actual half-cell temperature higher than the temperature measured by the thermocouple placed some distance ($\sim$5 mm) away from the half-cell. Herle and his co-workers observed that the actual cell temperature (with active cell area of 1 cm^2) at 1.0 A/cm^2 can be higher by 20–25 °C than at low current density, which is evidenced by their thermal modeling results [24, 25]. The change of ohmic resistance with bias current density increases the difficulty/complexity in the correction of ohmic-drop. Figure 8 shows electrode potential E ($E = i\ R_{ohm} + \eta$, electrode overpotential $\eta(\eta = E - i\ R_{ohm)}$ after ohmic-drop correction, ohmic resistance R_{ohm} and electrode polarization resistance R_p measured at 700 °C of LSM–GDC composite cathode as a function of bias current density. If the ohmic-drop is corrected based on the electrolyte ohmic resistance under open-circuit, the overpotential at current density above 400 mA/cm^2 would become negative. Thus, it is reasonable that the ohmic drop is corrected based on the corresponding electrolyte ohmic resistance under each bias current density. The overpotential measured at 700 °C of the LSM–GDC composite cathode in this study was $\sim$180 mV at 200 mA/cm^2, which is slightly higher than that of LSM–GDC composite cathode prepared by ion-impregnation method ($\sim$140 mV at 200 mA/cm^2 and $\sim$190 mV at 300 mA/cm^2) [20]. With increasing bias current density, the electrode polarization resistance decreases. The electrode polarization resistance under 200 mA/cm^2 and 1.0 A/cm^2 was $\sim$1.06 and 0.21 $\Omega\ cm^2$ at 700 °C, almost two and nine times smaller than that under open circuit ($\sim$1.87 $\Omega\ cm^2$ at 700 °C), respectively. The improvement of cathode performance at high bias current density was reported to be associated with the formation of oxygen vacancies [26, 27]. On the other hand,

the corresponding $i \times R_p$ is close to the overpotential at each current density. For example, $i \times R_p$ at 200 mA/cm^2 is $\sim$212 mV, close to the overpotential of $\sim$180 mV at the same current density. This indicates that the electrode polarization resistance R_p under bias current density can be used to evaluate the cathode performance.

To compare the polarization behavior of the LSM–GDC composite cathode with that of pure LSM cathode, the electrode polarization resistance of pure LSM was measured as a function of bias current density. Similar to the LSM–GDC composite cathode, the electrode polarization resistance of pure LSM cathode decreases with increasing bias current density, as shown in Fig. 9. The electrode polarization resistance of the LSM–GDC composite cathode measured at 700 °C under open-circuit condition is $\sim$1.87 $\Omega\ cm^2$, which is higher than that of pure LSM cathode measured at 850 °C under open-circuit ($\sim$1.17 $\Omega\ cm^2$). However, the electrode polarization resistance of the LSM–GDC composite cathode measured at 700 °C under 500 mA/cm^2 is almost the same as that of pure LSM cathode measured at 850 °C under the same current density ($\sim$0.42 $\Omega\ cm^2$). This implies that modification of LSM powders by $Gd_{0.2}Ce_{0.8}(NO_3)_x$ solution impregnation can effectively reduce the operating temperature of pure LSM cathodes by 150 °C while maintaining roughly the same cathode performance.

Conclusions

The LSM–GDC composite powder has been prepared by modifying the LSM powder with $Gd_{0.2}Ce_{0.8}(NO_3)_x$ nitrate solution impregnation, followed by calcination. $Gd_{0.2}Ce_{0.8}(NO_3)_x$ nitrate solution impregnation

modification of LSM powder can not only inhibit the growth of LSM grains during the sintering process but it also increases the TPB area by introducing an ionic conducting phase $(Gd,Ce)O_{2-\delta}$, leading to significant reduction of the electrode polarization of pure LSM cathode. At 750 °C, the cathode prepared from the LSM–GDC composite (GDC: 30 wt%) powder shows $\sim$13 times lower electrode polarization resistance ($\sim 0.60\ \Omega\ cm^2$ at 750 °C under open circuit) than that of pure LSM cathode ($\sim 8.19\ \Omega\ cm^2$ at 750 °C under open circuit) on YSZ electrolyte substrates. The electrode polarization resistance of the LSM–GDC composite cathode at 700 °C under 500 mA/cm² was $\sim 0.42\ \Omega\ cm^2$, which is close to that of pure LSM cathode at 850 °C under the same current density. This implies that $Gd_{0.2}Ce_{0.8}(NO_3)_x$ solution impregnation approach can effectively reduce the operating temperature of pure LSM cathodes by 150 °C while maintaining roughly the same cathode performance. The results demonstrate the feasibility of modifying the LSM powder with $Gd_{0.2}Ce_{0.8}(NO_3)_x$ nitrate solution impregnation in the development of high performance cathodes for inter-mediate-temperature SOFCs.

References

1. Souza SD, Visco SJ, Jonghe LCD (1997) Solid State Ionics 98:57
2. Kim JW, Virkar AV, Fung KZ, Mehta K, Singhal SC (1999) J Electrochem Soc 146:69
3. Leng YJ, Chan SH, Khor KA, Jiang SP, Cheang P (2003) J Power Sources 117:26
4. Maric R, Ohara S, Fukui T, Yoshida H, Nishimura M, Inagaki T, Miura K (1999) J Electrochem Soc 146:2006
5. Ishihara T, Shibayama T, Honda M, Nishiguchi H, Takita Y (2000) J Electrochem Soc 147:1332
6. Wang K, Wan JH, Goodenough JB (2001) J Electrochem Soc 148:A788
7. Yan JW, Lu LG, Jiang Y, Dong YL, Yu CL, Li WZ (2002) J Electrochem Soc 149:A1132
8. Doshi R, Richards VL, Carter JD, Wang X, Krumpelt M (1999) J Electrochem Soc 146:1273
9. Xia C, Chen F, Liu M (2001) Electrochem Solid State Lett 4:A52
10. Xia C, Liu M (2001) Solid State Ionics 144:249
11. Leng YJ, Chan SH, Jiang SP, Khor KA (2004) Solid State Ionics 170:9
12. Minh NQ (1993) J Am Ceram Soc 76:563
13. Steele BCH, Bae JM (1998) Solid State Ionics 106:255
14. Dusastre V, Kilner JA (1999) Solid State Ionics 126:163
15. Kim JD, Kim GD, Moon JW, Park YI, Lee WH, Kobayashi K, Nagai M, Kim CE (2001) Solid State Ionics 143:379
16. Jørgensen MJ, Primdahl S, Bagger C, Mogensen M (2001) Solid State Ionics 139:1
17. Murray EP, Tsai T, Barnett SA (1998) Solid State Ionics 110:235
18. Murray EP, Barnett SA (2001) Solid State Ionics 143:265
19. Xia C, Zhang Y, Liu M (2003) Electrochem Solid State Lett 6:A290
20. Jiang SP, Leng YJ, Chan SH, Khor KA (2003) Electrochem Solid State Lett 6:A67
21. Chen XJ, Chan SH, Khor KA (2004) Electrochim Acta 49:1851
22. Jiang SP, Love JG (2001) Solid State Ionics 138:183
23. Jiang SP, Love JG (2003) Solid State Ionics 158:45
24. Herle JV, Ihringer R, Cavieres RV, Constantin L, Bucheli O (2001) J Euro Ceram Sci 21:1855
25. Larrain D, Herle JV, Maréchal F, Favrat D (2003) J Power Sources 118:367
26. Jiang Y, Wang SZ, Zhang YH, Yan JW, Li WZ (1998) J Electrochem Soc 145:373
27. Lee HY, Cho WS, Oh SM, Wiemhöfer HD, Göpel W (1995) J Electrochem Soc 142:2659